

See discussions, stats, and author profiles for this publication at: <https://www.researchgate.net/publication/263955896>

Modeling Water Adsorption on Rutile (110) Using van der Waals Density Functional and DFT+U Methods

ARTICLE *in* THE JOURNAL OF PHYSICAL CHEMISTRY C · OCTOBER 2013

Impact Factor: 4.77 · DOI: 10.1021/jp404052k

CITATIONS

6

READS

22

4 AUTHORS, INCLUDING:



Nitin Kumar

University of Michigan

16 PUBLICATIONS 144 CITATIONS

SEE PROFILE



J. D. Kubicki

University of Texas at El Paso

216 PUBLICATIONS 4,438 CITATIONS

SEE PROFILE

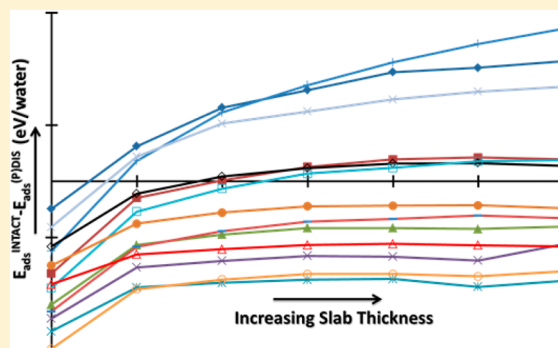
Modeling Water Adsorption on Rutile (110) Using van der Waals Density Functional and DFT+U Methods

Nitin Kumar,^{*,†,‡} Paul R. C. Kent,[§] David J. Wesolowski,^{||} and James D. Kubicki[‡]

[†]Department of Mechanical and Nuclear Engineering, and [‡]Department of Geosciences, The Pennsylvania State University, University Park, Pennsylvania 16802, United States

[§]Center for Nanophase Materials Sciences and Computer Science and Mathematics Division, and ^{||}Chemical Sciences Division, Oak Ridge National Laboratory, Oak Ridge, Tennessee 37830, United States

ABSTRACT: We study the energetics and structure of water absorption on the ideal rutile TiO_2 (110) surface using dispersion-corrected periodic density functional theory (DFT) calculations and on-site Coulomb potential (DFT+U) corrections. Conventional (PBE) and self-consistent dispersion-corrected DFT methods (vdw-DF1 and vdw-DF2) both suggest that molecular adsorption of intact water molecules on the rutile (110) surface is increasingly preferred with increasing simulation slab thickness. However, empirical dispersion corrections indicate a mix of molecular and dissociated water may coexist at room temperature, with less dependence on slab thickness. This same behavior is seen for DFT+U with $U = 3$ eV in combination with or without self-consistent dispersion corrected DFT. We find that the preference for the occurrence of dissociated water increases with increasing U . When compared with experimental bond-length data for the adsorbed water species, none of the methods and slab thicknesses correctly predict all bond lengths simultaneously. However, of the methods that energetically favor coexisting associated and dissociated water species on the surface, the three-layer slab with conventional DFT (PBE) and the empirically dispersion-corrected DFT methods come closest to correctly reproducing all of the experimentally observed bond lengths. We conclude that the current level of DFT is insufficient to definitively distinguish between the fully associated and partially dissociated states of water adsorbed on the pristine rutile (110) surface, due to the very small (~ 0.1 eV) total energy differences between these states.



INTRODUCTION

The nature of water adsorption on the ideal (110) surface of α - TiO_2 (rutile) remains a highly controversial topic.^{1–15} There have been numerous attempts, both experimentally^{1,4–8,15} and theoretically,^{1–3,9–14} to determine the dissociation state of the first layer of chemisorbed water molecules. In experiments, there have been disagreements about the possibility of any water dissociation on the ideal rutile (110) surface. Different studies have reported finding no dissociation^{4–6} to partial dissociation^{7,8,15} for this surface. This confusion is compounded by the theoretical studies where both partial^{9–13,16} and fully associated^{2,3,14} states are supported.

Prediction of the degree of water dissociation on rutile (110) using density functional theory is particularly challenging due to the many competing electronic interactions. The previous density functional theory (DFT) studies of the water/rutile (110) interface have mainly used local and gradient-corrected functionals. These functionals do not incorporate either dispersion (van der Waals) corrections or any special treatment for the d electrons of the Ti atoms, and the resultant self-interaction. These are both potential sources of error in the calculations. In addition, a high overall degree of accuracy is

required due to the small energy differences between associated and dissociated states, approximately 0.1 eV.

Although little guidance is available for selecting DFTs for the *interfacial* problem, it is well understood that conventional as well as hybrid DFTs fail to reproduce the *bulk* phase behavior of TiO_2 ^{17–19} polymorphs and their electronic structure.²⁰ The inclusion of empirical dispersion corrections correctly predicts rutile to be the most stable phase, at the expense of strongly polarizable oxygen atoms.¹⁸ Although this result might appear surprising, finite-size scaling analysis of the van der Waals energy of clusters and analysis of the bulk dielectric constants indicates the van der Waals contribution to the cohesive energy of solids can be significant.²¹ DFT+U has also been extensively explored, either to correct the phase diagram or to improve the electronic bandgap.^{17–20} Overall, these results indicate that dispersion and electron self-interaction corrections should be explored in these metal-oxide systems.

Received: April 24, 2013

Revised: October 15, 2013

Published: October 16, 2013



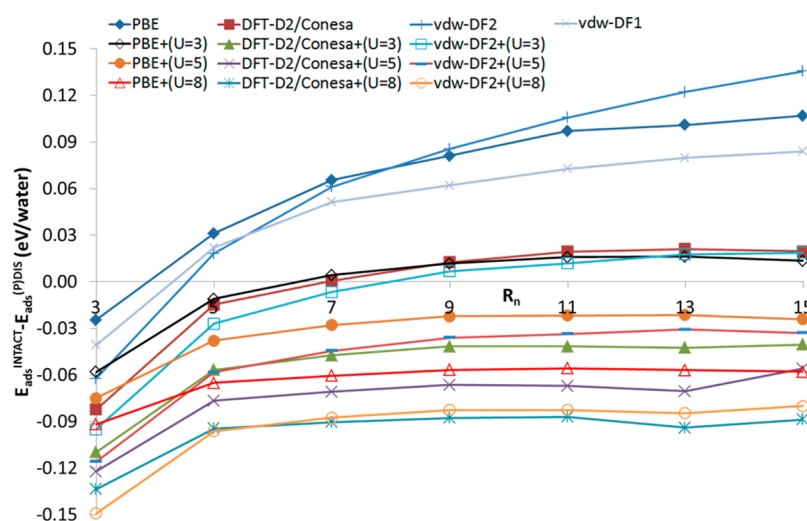


Figure 1. Adsorption energy difference (eV/water molecule) between associated (INTACT) and partially dissociated ((P)DIS) configurations using various dispersion and DFT+U corrections with varying slab thicknesses (R_3 – R_{15}). Negative energies indicate a preference for dissociated water. When using conventional PBE (blue solid tilted square), the energy difference increases monotonically with slab thickness without any sign of convergence. A similar energy profile (blue plus and times signs) is observed when fully self-consistent dispersion corrected density functional, i.e., vdW-DF1 and vdW-DF2,²⁵ scheme is used. However, the empirical version of the dispersion correction DFT-D2/Conesa^{18,22,23} scheme (red solid square) significantly reduces the energy difference between the fully associated and partially dissociated configurations, making both associated and dissociated water molecules to coexist at room temperature. DFT+U with $U = 3$ eV (black empty tilted square) and vdW-DF2 with $U = 3$ eV (blue empty square) produces a very similar energy profile as seen in the DFT-D2/Conesa scheme (red solid square). But the DFT-D2/Conesa with DFT+U correction, where $U = 3$ eV (green solid up triangle), results in an energy profile which indicates that partially dissociated water is the preferred mode of water adsorption for all slab thicknesses (R_3 – R_{15}). A similar preference for partially dissociated configuration was observed when U parameter is increased, i.e., $U = 5$ eV (orange solid circle), $U = 8$ eV (red empty up triangle) without any dispersion correction or with vdW-DF2 (blue line for $U = 5$ eV and orange empty circle for $U = 8$ eV) or with DFT-D2/Conesa (purple times sign for $U = 5$ eV and blue asterisk for $U = 8$ eV) dispersion correction. The preference for partially dissociated configuration strengthens as the U value increases, irrespective of whether any dispersion correction is included.

In this paper, we examine the influence of dispersion corrections on the dissociation state of chemisorbed water, using both the empirical scheme of Grimme^{22,23} (DFT-D2) and using the fully self-consistent density functional vdW-DF1 and vdW-DF2 scheme of Langreth and Lundqvist.^{24,25} We also examine the effect of correcting the on-site Coulomb interactions for the Ti atoms using a DFT+U scheme, separately and in combination with the dispersion corrected methods. Conventional density functionals are well-known to produce band gaps smaller than experiment for both bulk and surface TiO_2 . DFT+U is a cheap and pragmatic correction to the electronic structure description²⁰ that in part reduces the self-interaction error of d levels and also allows for their empirical parametrization (e.g., to match spectroscopic data). Note that dispersion corrections do not directly affect these electronic properties.²³ The U value to use depends on the specifics of the system under study. $U = 5$ or 8 eV has been shown to predict the correct phase stability for TiO_2 .¹⁷ However, $U = 3$ eV gives more accurate reaction energies for the oxidation of Ti_2O_3 to TiO_2 , which can be important for studying the catalytic properties of rutile.²⁰ $U = 3.5$ eV has been used for simulations of water on anatase TiO_2 .²⁶ In the end, we compare metal–oxygen bond lengths with experiments to assess the performance of the different methods.

METHOD

We used the Vienna ab initio Simulation Package (VASP)^{27–30} to perform the DFT calculations reported in this work. A frozen-core projector-augmented wave scheme^{31,32} was used to treat the core electrons, with the wave functions of the valence electrons expanded in a 500 eV plane wave basis set. The

PBE^{33,34} potential was used as gradient-corrected exchange–correlation functional. The rutile (110) surface was modeled as a periodic slab of (2×1) supercell and the Brillouin zone sampling used $2 \times 2 \times 1$ k-points. The central layer of the slab was kept fixed at the bulk rutile structure and all other atoms were relaxed until the forces on all relaxed atoms were below the convergence threshold of 0.01 eV/Å. Water molecules were adsorbed on both sides of the slab to maintain symmetry, with the vacuum separation between the two surfaces being around 15 Å. It has previously been established that the structure and energies of the bare surface and of adsorbed water is highly sensitive to slab thickness.^{1–3}

The sensitivity of our results to the parameters used in the calculations was tested for the thick slab R_7 . Cut-off energies of 400, 500, 800, and 1250 eV were checked, and an additional set of calculations performed with $4 \times 4 \times 2$ k-points. We also checked the vacuum thickness dependence of results where the vacuum separation between the slabs was changed from 15 to 20, 25, and 30 Å, respectively. In all of these other calculations, the energy was found to be converged with the difference being of the order of 0.002, 0.003, and 0.001 eV for energy cutoff, k-points, and vacuum separation parameters, respectively. Moreover, the bond lengths were found to converge within 0.001 Å for the range of energies considered above. As will be seen below, the energy convergence and the bond length convergence error is much smaller than the corresponding energy and bond length differences due to the use of different density functionals.

The dispersion interaction correction to DFT, as proposed by Grimme,^{22,23} was used with the van der Waals parameters for Ti and O developed by Conesa¹⁸ to stabilize the rutile

phase, denoted as DFT-D2/Conesa. Other details were given by Grimme et al.^{22,23} It is important to note that the DFT-D2/Conesa method uses empirical parameters that were trained for the bulk rutile phase.¹⁸ The interface presents a significantly different local environment, such as water molecules either in associated or dissociated state. Hence, an ideal application of DFT-D2/Conesa method requires determination of empirical parameters in the interfacial environment. This study will be undertaken in future work. The fully self-consistent dispersion correction, denoted as vdW-DF1 and vdW-DF2, was used as implemented^{24,25} in VASP. vdW-DF1 and vdW-DF2 method uses optPBE and rPW86 exchange functional, respectively. The DFT+U³⁵ was implemented on the d shell of the Ti atom for a range of U parameters $U = 0, 3, 5$, or 8 eV.^{17,20}

RESULTS

On the rutile (110) surface, the first layer of water molecules can chemisorb on the dry surface molecularly, known as the associated configuration. The corresponding water molecule is known as terminal water (TW), which adsorbs atop under-coordinated Ti atoms exposed on the vacuum-terminated (110) surface. This water molecule can also dissociate with one of the H-atoms migrating to a neighboring bridging oxygen (BO), which is known as the dissociated configuration. The dissociated water molecule is referred to as terminal hydroxyl (TH), and the protonated BO is known as bridging hydroxyl (BH). In our simulation, the 2×1 surface unit cells allow chemisorption of two water molecules in the first layer. A partially dissociated configuration is defined for this study when one of these water molecules dissociates, leading to a 1:1 mixture of associated and dissociated water molecules on the surface. In Figure 1, we show the adsorption total energy difference between fully associated and partially dissociated configurations with varying slab thicknesses (R_3 – R_{15}) for various DFT methods. Using conventional PBE (Figure 1), as R_n is increased from R_3 to R_5 , it becomes energetically favorable for the adsorbed water molecules to be in the fully associated configuration, at least in terms of system total energy, which neglects entropic effects. Liu et al.³ reported similar behavior for this interface. The adsorption total energy difference between the associated and partially dissociated configurations for R_3 surface is -0.02 eV/water molecule, whereas it is $+0.03$ eV/water molecule for R_5 . The energy difference increases monotonically for thicker slabs (symmetrical, odd-numbered slabs only considered here), and it does not appear to converge even for the thickest slab, that is, R_{15} , considered in the present study. Liu et al.³ demonstrated similar slow convergence for both odd and even thickness asymmetric slabs (water on one side only).

We now consider the effect of dispersion corrections. The DFT-D2/Conesa description of dispersion, Figure 1, significantly changes the dependence of the adsorption energy difference with slab thickness. Both R_3 and R_5 slabs are found to prefer a partially dissociated configuration for the adsorbed water molecules. The adsorption energy difference diminishes for the R_7 slab geometry, indicating that both molecular and dissociated water molecules can coexist. As the slab thickness is further increased from R_9 to R_{15} , the associated configuration is slightly preferred (energy difference of 0.01 to 0.02 eV) over the partially dissociated configuration. The small energy difference between the two configurations indicates that, at room temperature (~ 0.025 eV), the water/rutile (110) surface

will have both associated and dissociated configurations coexisting, due to thermal fluctuations, for all slab thicknesses (R_3 – R_{15}).

The self-consistent vdW-DF1 and vdW-DF2 functional, Figure 1, predicts a similar adsorption energy profile to the PBE result. Moreover, the adsorption energy from this method increases monotonically with a much higher tendency to diverge (“nonconvergence”) than the PBE result. It is interesting to note that the two van der Waals methods yield very different results. The DFT-D2/Conesa method indicates that the rutile (110) surface will have a partially dissociated surface for all slab thicknesses at room temperature. On the other hand, both vdW-DF1 and vdW-DF2 finds that as thicker slabs are considered the rutile (110) surface preference for fully associated water molecules increases, with even less convergence than was observed for PBE. It is important to note that the DFT-D2/Conesa^{22,23} method uses empirical parameters that are trained from the bulk rutile phase and are not sensitive to the local environment, while both vdW-DF1 and vdW-DF2 method is a fully self-consistent density functional able to compensate for surface effects, polarization, and charge transfer. This suggests that both vdW-DF1 and vdW-DF2 results are likely to be more reliable. Thus, the prediction from purely dispersion-corrected simulation is that the rutile (110) surface prefers to have adsorbed water molecules in associated configuration.

Next, we consider the effect of applying DFT+U over a range of U values ($3 \leq U \leq 8$ eV) in conjunction with the PBE functional. Surprisingly, we find that the energy profile for PBE + $U = 3$ eV (Figure 1) follows very closely to that predicted by the empirical DFT-D2/Conesa method (implicitly with $U = 0$ eV). However, as the U value is increased to $U = 5$ eV or $U = 8$ eV, the rutile surface preference completely changes to partially dissociated configurations for all slab thicknesses (R_3 – R_{15}). If DFT+U is combined with the DFT-D2/Conesa corrections for $U = 3, 5$, and 8 eV, respectively, the rutile (110) surface continues to maintain its strong preference toward partial dissociation. Although rarely tested or used in combination, if DFT+U is combined with the vdW-DF2 method, the tendency toward dissociation becomes stronger. The vdW-DF2 with $U = 3$ eV results in an energy profile very similar to the DFT+U, with $U = 3$ eV (Figure 1), or the empirical DFT-D2/Conesa with $U = 0$ eV (Figure 1) method. Thus, as soon as DFT+U correction is turned on, irrespective of whether any dispersion correction is included or not, the rutile (110) surface’s tendency changes to having both associated and dissociated configurations possible at room temperature. It is also interesting to note that as the on-site Coulomb repulsion in the d orbitals is increased (increasing U parameter) the preference for partially dissociated configurations becomes stronger for all slab thicknesses (R_3 – R_{15}).

This study shows that the difference in energy between the fully associated and partially dissociated surface configurations is highly dependent on the DFT functional used, as well as the slab thickness used in the simulation, as previously reported.³ In order to identify the combinations that most closely reproduce the experimentally determined properties of ideal rutile (110), we have compared quantities such as the experimental metal–oxygen bond lengths for the adsorbed water molecules with those predicted by theory.

We have calculated the bond length between the oxygen atom of a TW, TH, BO, or BH, and the corresponding underlying metal atom, that is, $d(\text{Ti}–\text{O}_{\text{TW}})$, $d(\text{Ti}–\text{O}_{\text{TH}})$, $d(\text{Ti}–$

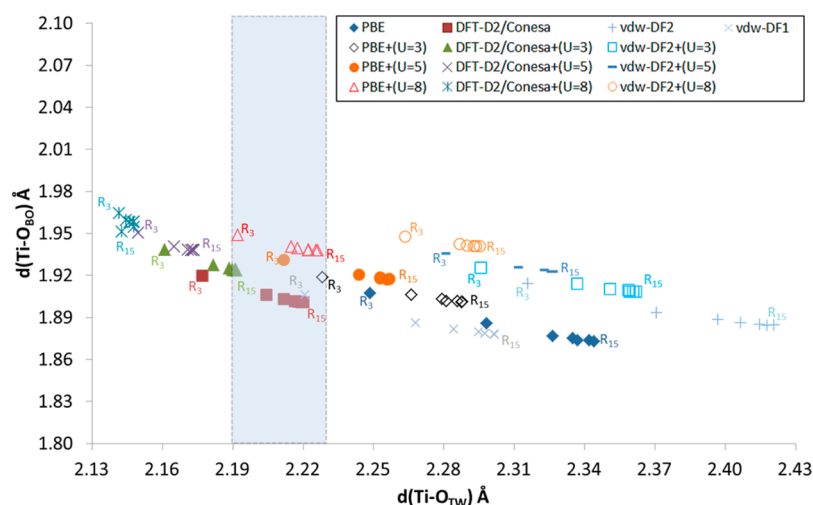


Figure 2. Metal oxygen bond length of bridging oxygen $\{d(\text{Ti}-\text{O}_{\text{BO}})\}$ vs terminal water $\{d(\text{Ti}-\text{O}_{\text{TW}})\}$ with varying slab thicknesses (R_3 – R_{15}) from various DFT methods. The shaded region shows the $d(\text{Ti}-\text{O}_{\text{TW}})$ bond length, 2.21 ± 0.02 Å, as determined experimentally by Allegretti et al.^{5,6} Among the many DFT methods and slab thicknesses considered in the present study, there are only few that correctly give $d(\text{Ti}-\text{O}_{\text{TW}})$ within the experimental range. These are vdw-DF1 (blue times sign) for R_3 , DFT-D2/Conesa (red solid square) for R_5 – R_{15} , DFT-D2/Conesa with $U = 3$ eV (green solid up triangle) for R_7 – R_{15} , DFT+U with $U = 3$ eV (black empty tilted square) for R_3 , DFT+U with $U = 5$ eV (orange solid circle) for R_3 , and DFT+U with $U = 8$ eV (red empty up triangle) for R_3 – R_{15} . However, DFT-D2/Conesa with $U = 5$ and 8 eV (purple times sign and blue asterisk) for R_3 – R_{15} , DFT-D2/Conesa with $U = 3$ eV (green solid up triangle) for R_3 – R_5 , and DFT-D2/Conesa (red solid square) for R_3 underestimates the $d(\text{Ti}-\text{O}_{\text{TW}})$. All other methods and slab thicknesses overestimate the $d(\text{Ti}-\text{O}_{\text{TW}})$. It is interesting to find that the methods which predicts the $d(\text{Ti}-\text{O}_{\text{TW}})$ bond length within the experimental range also favor partial dissociation of the adsorbed water molecule at room temperature. R_3 and R_{15} symbols, in the plot above, correspond to two extremes of the slab thickness considered in this work.

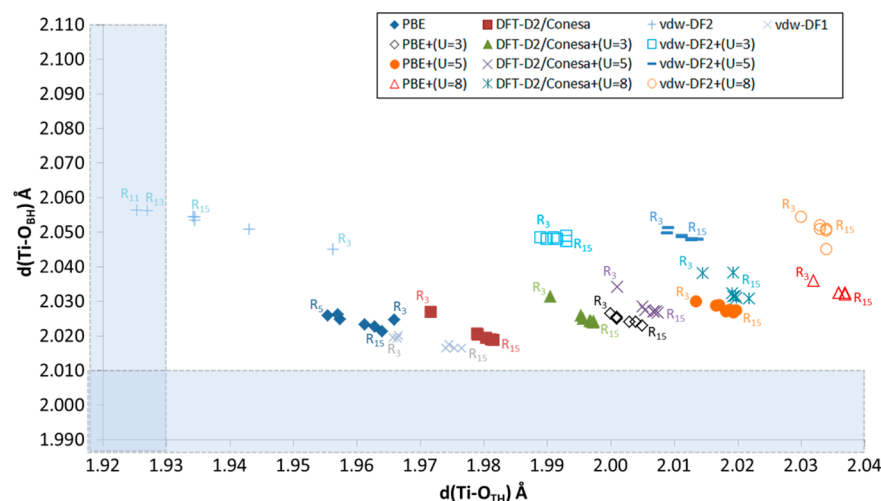


Figure 3. Metal oxygen bond length of bridging hydroxyl $\{d(\text{Ti}-\text{O}_{\text{BH}})\}$ vs terminal hydroxyl $\{d(\text{Ti}-\text{O}_{\text{TH}})\}$ with varying slab thicknesses (R_3 – R_{15}) from various DFT methods. The shaded region corresponds to experimentally determined bond lengths by Duncan et al.¹⁵ They report the $d(\text{Ti}-\text{O}_{\text{BH}})$ and $d(\text{Ti}-\text{O}_{\text{TH}})$ to be 1.94 ± 0.07 Å and 1.85 ± 0.08 Å, respectively. It is clear that none of the DFT methods with any slab thickness, that are studied in the present work, correctly predicts the $d(\text{Ti}-\text{O}_{\text{BH}})$. Only slabs R_{11} and R_{13} with vdw-DF2 (blue plus sign) correction predicts $d(\text{Ti}-\text{O}_{\text{TH}})$ within the experimental range. However, this combination of slab thickness and DFT method severely overestimates the $d(\text{Ti}-\text{O}_{\text{BH}})$ (Figure 2). R_3 and R_{15} symbols correspond to two extremes of the slab thickness considered in this work.

O_{BO}), and $d(\text{Ti}-\text{O}_{\text{BH}})$, respectively, for all DFT methods discussed above. Figure 2 shows a plot of $d(\text{Ti}-\text{O}_{\text{BO}})$ vs $d(\text{Ti}-\text{O}_{\text{TW}})$ for the range of slab thicknesses (R_3 – R_{15}) from various DFT methods. The shaded region in Figure 2 corresponds to $d(\text{Ti}-\text{O}_{\text{TW}})$ as determined from the scanned-energy mode photoelectron diffraction (PhD) experimental approach reported by Allegretti et al.^{5,6} In general, calculated $d(\text{Ti}-\text{O}_{\text{TW}})$ increases and $d(\text{Ti}-\text{O}_{\text{BO}})$ decreases as the slab thickness is increased from R_3 to R_{15} for all DFT methods, with $d(\text{Ti}-\text{O}_{\text{BO}})$ less sensitive to DFT method or slab thickness. A comparison with this experiment clearly shows that vdw-DF1

for R_3 , DFT-D2/Conesa for R_5 – R_{15} , DFT-D2/Conesa with $U = 3$ eV for R_7 – R_{15} , PBE+U with $U = 3$ eV for R_3 , PBE+U with $U = 5$ eV for R_3 , and PBE+U with $U = 8$ eV for R_3 – R_{15} all predict the $d(\text{Ti}-\text{O}_{\text{TW}})$ to within the experimental error. In contrast, DFT-D2/Conesa with $U = 5$ and 8 eV for R_3 – R_{15} , DFT-D2/Conesa with $U = 3$ eV for R_3 – R_5 , and DFT-D2/Conesa for R_3 underestimate the $d(\text{Ti}-\text{O}_{\text{TW}})$ bond length. All other DFT methods and slab thickness combinations overestimate the $d(\text{Ti}-\text{O}_{\text{TW}})$ bond length, with vdw-DF2 with no U correction giving the largest deviation. A comparison of Figures 1 and 2 demonstrates that the methods that correctly

Table 1. Total Absolute Error for Ti–O Bond Lengths When Predicted Bond Lengths Are Compared with the Experiments^a

R_n	PBE	PBE+ ($U = 3$)	PBE+ ($U = 5$)	PBE+ ($U = 8$)	DFT-D2/ Conesa	DFT-D2/ Conesa+ ($U = 3$)	DFT-D2/ Conesa+ ($U = 5$)	DFT-D2/ Conesa+ ($U = 8$)	vdw- DF2	vdw- DF2+ ($U = 3$)	vdw- DF2+ ($U = 5$)	vdw- DF2+ ($U = 8$)	vdw- DF1
3	0.07	0.09	0.10	0.13	0.07	0.11	0.14	0.16	0.15	0.17	0.17	0.18	0.06
5	0.11	0.12	0.12	0.13	0.06	0.09	0.12	0.16	0.19	0.21	0.20	0.20	0.08
7	0.14	0.14	0.13	0.13	0.06	0.08	0.11	0.15	0.21	0.22	0.21	0.20	0.10
9	0.15	0.14	0.13	0.13	0.06	0.08	0.11	0.15	0.23	0.23	0.22	0.21	0.12
11	0.15	0.14	0.13	0.13	0.06	0.08	0.11	0.16	0.23	0.23	0.22	0.21	0.12
13	0.16	0.15	0.13	0.13	0.06	0.08	0.11	0.15	0.24	0.23	0.22	0.21	0.12
15	0.16	0.15	0.13	0.13	0.06	0.08	0.11	0.16	0.24	0.23	0.22	0.20	0.12

^aThe total absolute error is calculated by adding the absolute errors for all three metal–oxygen bond lengths, i.e., $d(\text{Ti}-\text{O}_{\text{TW}})$, $d(\text{Ti}-\text{O}_{\text{TH}})$, and $d(\text{Ti}-\text{O}_{\text{BH}})$. The numbers shown in bold correspond to those methods and slab thickness combinations which do not energetically favor the partially dissociated configuration at room temperature.

predict $d(\text{Ti}-\text{O}_{\text{TW}})$ also energetically favor partial dissociation at room temperature.

Allegretti et al.^{5,6} reported the presence of only associated water molecules atop rutile (110) surface, but, recently the Allegretti group,¹⁵ reported that both associated and dissociated water molecules coexist on this surface, and were able to distinguish between BH hydroxyls produced by reaction of water molecules with oxygen vacancies (a common defect in rutile (110) surfaces exposed to ultrahigh vacuum) and BH–TH pairs resulting from TW dissociation on the pristine (non-defective) surface. Moreover, this claim was also supported in an independent work by Walle et al.⁸ The dissociation process produces terminal hydroxyls which have shorter metal–oxygen bond lengths than their nondissociated counterparts, which was also reported from X-ray reflectivity studies of the contact between bulk liquid water and rutile single crystals exposing the (110) surface.⁷

Figure 3 shows the plot of $d(\text{Ti}-\text{O}_{\text{BH}})$ versus $d(\text{Ti}-\text{O}_{\text{TH}})$ for partially dissociated configurations with varying slab thicknesses (R_3 – R_{15}) from various DFT methods. The shaded regions show the experimentally determined bond lengths.¹⁵ Only the vdW-DF2 ($U = 0$ eV) method for R_{11} and R_{13} slabs, which energetically favors no dissociation on thick slabs (Figure 1), gives $d(\text{Ti}-\text{O}_{\text{TH}})$ bond lengths in agreement with experiment. However, this method overestimates $d(\text{Ti}-\text{O}_{\text{BH}})$ by the largest margin of all methods tested. In fact, none of the methods and slab thicknesses considered in the present study correctly predict $d(\text{Ti}-\text{O}_{\text{BH}})$, compared with the experimental result.¹⁵

Table 1 shows the absolute total error (difference between theoretical prediction and experimental observation) for all three metal–oxygen bond lengths, $d(\text{Ti}-\text{O}_{\text{TW}})$, $d(\text{Ti}-\text{O}_{\text{TH}})$, and $d(\text{Ti}-\text{O}_{\text{BH}})$, summed together. Table 1 as well as Figures 2 and 3 clearly show that none of the methods and slab thicknesses considered in this work correctly predict all three bond lengths, simultaneously. Ideally, one or several methods would predict all bond lengths in agreement with experiment for large slab thicknesses. Note, however, that the pure PBE method for $R = 3$, vdW-DF1 for $R = 3$, and the DFT-D2/Conesa method at all slab thicknesses is closest to predicting all three bond lengths correctly (Table 1, Figures 2 and 3). Note also that the DFT methods that do not energetically favor partial dissociation at room temperature (pure PBE at $R > 5$, vdW-DF1 for $R > 5$, and vdW-DF2 without U correction at $R > 5$) appear to give bond lengths that, in sum, have large deviation from experimental results (Table 1). However, the agreement with experiment obtained for the thinner slab configurations must result from cancelation of errors, since the slab thickness effects are very large, particularly for R_3 .

DFT-MD simulations^{3,12,13} indicate that the metal–oxygen bond lengths are sensitive to the presence of additional water above the surface. Zhang et al.⁷ used X-ray crystal truncation rod (CTR) method to determine the Ti–O bond lengths for macroscopic rutile (110) single-crystal surfaces submerged in bulk water. The bond lengths correspond to an average between hydroxylated and nonhydroxylated O because the H atoms are nearly invisible in X-rays. Hence, in this experiment, for example, the $d(\text{Ti}-\text{O}_{\text{TO}})$ actually corresponds to an average of $d(\text{Ti}-\text{O}_{\text{TW}})$ and $d(\text{Ti}-\text{O}_{\text{TH}})$. The X-ray CTR study⁷ reported the $d(\text{Ti}-\text{O}_{\text{TO}})$ and $d(\text{Ti}-\text{O}_{\text{BO}})$ to be 2.13 ± 0.03 Å and 1.95 ± 0.02 Å, respectively, at pH ≈ 5.5 (pure water equilibrated with atmospheric CO_2). At this pH, the surface protonation scheme for rutile (110) in contact with bulk water developed by Wesolowski and co-workers (summarized in ref 1) predicts the surface to be $\sim 75\%$ associated, suggesting that these observed bond lengths are close to the $d(\text{Ti}-\text{O}_{\text{TW}})$ and $d(\text{Ti}-\text{O}_{\text{BO}})$ bond lengths, respectively. Interestingly, this level of TW dissociation to TH–BH pairs was also reported by Duncan et al.¹⁵ at submonolayer water coverage. We have performed ab initio molecular dynamics (DFT-MD) simulations, using PBE, on an R_3 slab^{1,12,13} with two additional layers of water above the hydrated rutile (110) surface. We found $d(\text{Ti}-\text{O}_{\text{TO}})$ and $d(\text{Ti}-\text{O}_{\text{BO}})$ to be 2.15 and 1.94 Å, respectively, which are in excellent agreement with the X-ray CTR result.⁷ Note that DFT-MD simulations (using PBE) with an R_4 asymmetrical slab (water on one side only)³ with several additional water layers also predict a $d(\text{Ti}-\text{O}_{\text{TW}})$ of 2.1 Å, in agreement with the X-ray CTR study.⁷

We recognize that a rigorous assessment of the most favored state should be based on Gibbs free energy. However, we note that, whatever the magnitude of the entropic term, it should favor a mixed state of associated and dissociated adsorbed water. Hence, if the energy difference between the associated and dissociated states is small then entropy would further push the system toward the mixed state rather than the purely associated state. In order to get an estimate, we calculated the vibrational entropy for R_3 with PBE method and found that the dissociated configuration was preferred over associated configuration by 0.84 kJ at $T = 300$ K. An inclusion of configurational entropy will further push the system toward dissociated configuration.

CONCLUSION

We have investigated the adsorption preference of water on the rutile (110) surface using a broad range of DFT methods for a range of slab thicknesses (R_3 – R_{15}). We find that both

conventional PBE and the self-consistent vdW-DF1 and vdW-DF2 dispersion correction method indicate, as shown previously for PBE and other nondispersion corrected DFT methods (see ref 3 and previous theoretical studies cited therein), that as the slab thickness is increased the rutile (110) surface shows stronger preference toward the fully associated configuration. However, the preference for dissociation changes significantly when the empirical DFT-D2/Conesa dispersion correction is used, which indicates that, at room temperature (corresponding to ~ 0.025 eV), the rutile (110) surface will have a mix of both associated and dissociated configurations, due to thermal fluctuations. This same behavior is also seen when DFT+U correction with $U = 3$ eV is included for all DFT methods tested. Furthermore, we find that, as the U parameter increases above 3 eV, the preference for the partially dissociated configuration becomes stronger for all slab thicknesses (R_3 – R_{15}). Next, we compared metal oxygen bond lengths between various DFT methods and experiments. We find that none of the methods and slab thicknesses correctly estimate all three Ti–O bond lengths for the TW, TH, and BH species that were determined experimentally.^{5,6,15} Of the methods that energetically favor mixed associated/dissociated surface water species, the R_3 slab using pure PBE without any dispersion or DFT+U correction, vdW-DF1 for R_3 , and the DFT-D2/Conesa method ($U = 0$ or 3) for all slab thicknesses predict all bond lengths reasonably close to that determined experimentally. We also find an excellent agreement for the metal–oxygen bond lengths between our previous DFT-MD (PBE) simulations^{1,12,13} with R_3 slab with two additional water layers compared with bond lengths determined by the X-ray CTR study⁷ of bulk water in contact with a rutile (110) single-crystal surface. Significant error cancellation must be occurring in the PBE- R_3 simulations to produce the good agreement with experiments.

This study emphasizes the importance of small variations in calculated energy (on the order of 0.1 eV) in the prediction of interfacial water structure and speciation on the rutile (110) surface. A substantial body of experimental evidence points to partial dissociation of water at this surface, though other experimental results indicate little or no dissociation. The PBE functional alone, and the explicit van der Waals treatment (vdW-DF2) indicate that the associated state is energetically favored on sufficiently thick slabs. However, it must be kept in mind that these DFT methods do not adequately predict the experimentally observed TiO_2 phase diagram,^{17–19} bulk band gaps,²⁰ or surface Ti–O bond lengths of rutile (110) at monolayer sorbed-water coverages. Furthermore, the difference in total energy calculated from the current application of these methods is not the same as the difference in free energy, which also includes entropic effects and other considerations. Finally, “reasonable” corrections applied to both PBE and vdW-DF2 functionals, to treat dispersion and d-electron self-interactions, shift the energetics in favor of the partially dissociated state. The overall conclusion of this study is that the degree of water dissociation on the pristine rutile (110) surface remains ambiguous, and that the current level of density functional theory is inadequate to resolve this ongoing debate.

AUTHOR INFORMATION

Corresponding Author

*Tel: 505-284-9785. E-mail: nitinkr@umich.edu.

Present Address

[†]N.K.: Walter E Lay Automotive Lab, Room G029, University of Michigan, Ann Arbor, MI 48109-2125.

Notes

The authors declare no competing financial interest.

ACKNOWLEDGMENTS

We would like to thank Dr. Jorge O. Sofo for helpful discussions and suggestions throughout this work. This work was supported by the Division of Chemical Sciences, Geosciences and Biosciences, Office of Basic Energy Sciences, U.S. Department of Energy. Work by P.R.C.K. was conducted at the Center for Nanophase Materials Sciences, which is sponsored at Oak Ridge National Laboratory by the Scientific User Facilities Division, Office of Basic Energy Sciences, U.S. Department of Energy. Computational support was provided by the Research Computation and Cyberinfrastructure group at The Pennsylvania State University.

REFERENCES

- (1) Wesolowski, D. J.; et al. Comment on “Structure and Dynamics of Liquid Water on Rutile $\text{TiO}_2(110)$ ”. *Phys. Rev. B* **2012**, *85*, 167401.
- (2) Liu, L.-M.; Zhang, C.; Thornton, G.; Michaelides, A. Reply to ‘Comment on “Structure and Dynamics of Liquid Water on Rutile $\text{TiO}_2(110)$ ”’. *Phys. Rev. B* **2012**, *85*, 167402.
- (3) Liu, L.-M.; Zhang, C.; Thornton, G.; Michaelides, A. Structure and Dynamics of Liquid Water on Rutile $\text{TiO}_2(110)$. *Phys. Rev. B* **2010**, *82*, 161415.
- (4) Henderson, M. A. An HREELS and TPD Study of Water on $\text{TiO}_2(110)$: The Extent of Molecular Versus Dissociative Adsorption. *Surf. Sci.* **1996**, *355*, 151–166.
- (5) Allegretti, F.; O’Brien, S.; Polcik, M.; Sayago, D. I.; Woodruff, D. P. Adsorption Bond Length for H_2O on $\text{TiO}_2(110)$: A Key Parameter for Theoretical Understanding. *Phys. Rev. Lett.* **2005**, *95*, 226104.
- (6) Allegretti, F.; O’Brien, S.; Polcik, M.; Sayago, D. I.; Woodruff, D. P. Quantitative Determination of the Local Structure of H_2O on $\text{TiO}_2(110)$ Using Scanned-Energy Mode Photoelectron Diffraction. *Surf. Sci.* **2006**, *600*, 1487–1496.
- (7) Zhang, Z.; et al. Structure of Rutile $\text{TiO}_2(110)$ in Water and 1 Molal Rb^+ at pH 12: Inter-Relationship Among Surface Charge, Interfacial Hydration Structure, and Substrate Structural Displacements. *Surf. Sci.* **2007**, *601*, 1129–1143.
- (8) Walle, L. E.; Borg, A.; Uvdal, P.; Sandell, A. Experimental Evidence for Mixed Dissociative and Molecular Adsorption of Water on a Rutile $\text{TiO}_2(110)$ Surface Without Oxygen Vacancies. *Phys. Rev. B* **2009**, *80*, 235436.
- (9) Goniakowski, J.; Gillan, M. J. The Adsorption of H_2O on TiO_2 and $\text{SnO}_2(110)$ Studied by First-Principles Calculations. *Surf. Sci.* **1996**, *350*, 145–158.
- (10) Lindan, P. J. D.; Harrison, N. M.; Gillan, M. J. Mixed Dissociative and Molecular Adsorption of Water on the Rutile (110) Surface. *Phys. Rev. Lett.* **1998**, *80*, 762–765.
- (11) Zhang, C. J.; Lindan, P. J. D. Multilayer Water Adsorption on Rutile $\text{TiO}_2(110)$: A First-Principles Study. *J. Chem. Phys.* **2003**, *118*, 4620–4630.
- (12) Kumar, N.; et al. Hydrogen Bonds and Vibrations of Water on (110) Rutile. *J. Phys. Chem. C* **2009**, *113*, 13732–13740.
- (13) Kumar, N.; et al. Faster Proton Transfer Dynamics of Water on SnO_2 Compared to TiO_2 . *J. Chem. Phys.* **2011**, *134*, 044706.
- (14) Harris, L. A.; Quong, A. A. Molecular Chemisorption as the Theoretically Preferred Pathway for Water Adsorption on Ideal Rutile $\text{TiO}_2(110)$. *Phys. Rev. Lett.* **2004**, *93*, 086105.
- (15) Duncan, D. A.; Allegretti, F.; Woodruff, D. P. Water Does Partially Dissociate on the Perfect $\text{TiO}_2(110)$ Surface: A Quantitative Structure Determination. *Phys. Rev. B* **2012**, *86*, 045411.
- (16) Bates, S. P.; Kresse, G.; Gillan, M. J. The Adsorption and Dissociation of ROH Molecules on $\text{TiO}_2(110)$. *Surf. Sci.* **1998**, *409*, 336–349.
- (17) Arroyo-de Dompablo, M. E.; Morales-García, A.; Taravillo, M. DFT+U Calculations of Crystal Lattice, Electronic Structure, and

Phase Stability Under Pressure of TiO₂ Polymorphs. *J. Chem. Phys.* **2011**, *135*, 054503.

(18) Conesa, J. C. The Relevance of Dispersion Interactions for the Stability of Oxide Phases. *J. Phys. Chem. C* **2010**, *114*, 22718–22726.

(19) Ma, X. G.; et al. Pressure-Induced Phase Transition and Elastic Properties of TiO₂ Polymorphs. *Phys. Status Solidi B* **2009**, *246*, 2132–2139.

(20) Hu, Z.; Metiu, H. Choice of U for DFT+U Calculations for Titanium Oxides. *J. Phys. Chem. C* **2011**, *115*, 5841–5845.

(21) Zhang, G.-X.; Tkatchenko, A.; Paier, J.; Appel, H.; Scheffler, M. Van der Waals Interactions in Ionic and Semiconductor Solids. *Phys. Rev. Lett.* **2011**, *107*, 245501.

(22) Grimme, S. Semiempirical GGA-Type Density Functional Constructed with a Long-Range Dispersion Correction. *J. Comput. Chem.* **2006**, *27*, 1787–1799.

(23) Grimme, S.; Antony, J.; Ehrlich, S.; Krieg, H. A Consistent and Accurate Ab Initio Parametrization of Density Functional Dispersion Correction (DFT-D) for the 94 Elements H-Pu. *J. Chem. Phys.* **2010**, *132*, 154104.

(24) Dion, M.; Rydberg, H.; Schröder, E.; Langreth, D. C.; Lundqvist, B. I. Van der Waals Density Functional for General Geometries. *Phys. Rev. Lett.* **2004**, *92*, 246401.

(25) Klimeš, J.; Bowler, D. R.; Michaelides, A. Van der Waals Density Functionals Applied to Solids. *Phys. Rev. B* **2011**, *83*, 195131.

(26) Tilocca, A.; Selloni, A. DFT-GGA and DFT+U Simulations of Thin Water Layers on Reduced TiO₂ Anatase. *J. Phys. Chem. C* **2012**, *116*, 9114–9121.

(27) Kresse, G.; Hafner, J. Ab Initio Molecular-Dynamics Simulation of the Liquid-Metal amorphous-Semiconductor Transition in Germanium. *Phys. Rev. B* **1994**, *49*, 14251–14251.

(28) Kresse, G.; Hafner, J. Ab Initio Molecular Dynamics for Liquid Metals. *Phys. Rev. B* **1993**, *47*, 558–558.

(29) Kresse, G.; Furthmüller, J. Efficient Iterative Schemes for Ab Initio Total-Energy Calculations Using a Plane-Wave Basis Set. *Phys. Rev. B* **1996**, *54*, 11169–11169.

(30) Kresse, G.; Furthmüller, J. Efficiency of Ab-Initio Total Energy Calculations for Metals and Semiconductors Using a Plane-Wave Basis Set. *Comput. Mater. Sci.* **1996**, *6*, 15–50.

(31) Kresse, G.; Joubert, D. From Ultrasoft Pseudopotentials to the Projector Augmented-Wave Method. *Phys. Rev. B* **1999**, *59*, 1758.

(32) Blöchl, P. E. Projector Augmented-Wave Method. *Phys. Rev. B* **1994**, *50*, 17953.

(33) Perdew, J. P.; Burke, K.; Ernzerhof, M. Generalized Gradient Approximation Made Simple [Phys. Rev. Lett. 77, 3865 (1996)]. *Phys. Rev. Lett.* **1997**, *78*, 1396–1396.

(34) Perdew, J. P.; Burke, K.; Ernzerhof, M. Generalized Gradient Approximation Made Simple. *Phys. Rev. Lett.* **1996**, *77*, 3865.

(35) Dudarev, S. L.; Botton, G. A.; Savrasov, S. Y.; Humphreys, C. J.; Sutton, A. P. Electron-Energy-Loss Spectra and the Structural Stability of Nickel Oxide: An LSDA+U Study. *Phys. Rev. B* **1998**, *57*, 1505.